



HAL
open science

Estimating the effect of operational loading condition from ultrasonic guided wave measurements using an iterated Unscented Kalman Filter

Andre Dalmora, Alexandre Imperiale, Sébastien Imperiale, Philippe Moireau

► To cite this version:

Andre Dalmora, Alexandre Imperiale, Sébastien Imperiale, Philippe Moireau. Estimating the effect of operational loading condition from ultrasonic guided wave measurements using an iterated Unscented Kalman Filter. 3ème colloque du GDR MecaWave, May 2023, Porquerolles, France. cea-04272530

HAL Id: cea-04272530

<https://cea.hal.science/cea-04272530>

Submitted on 6 Nov 2023

HAL is a multi-disciplinary open access archive for the deposit and dissemination of scientific research documents, whether they are published or not. The documents may come from teaching and research institutions in France or abroad, or from public or private research centers.

L'archive ouverte pluridisciplinaire **HAL**, est destinée au dépôt et à la diffusion de documents scientifiques de niveau recherche, publiés ou non, émanant des établissements d'enseignement et de recherche français ou étrangers, des laboratoires publics ou privés.

DA1



Estimating the effect of operational loading conditions from ultrasonic guided wave measurements using an iterated Unscented Kalman Filter

André Luiz Dalmora^{1,2,3}, Alexandre Imperiale¹, Sébastien Imperiale^{2,3}, Philippe Moireau^{2,3}

¹ Université Paris-Saclay, CEA, List, F-91120, Palaiseau, France

² Project-Team M3DISIM, Inria Saclay-Ile-de-France, Inria, 91128 Palaiseau, France

³ LMS, École Polytechnique, CNRS, Institut Polytechnique de Paris, 91128 Palaiseau, France

10/05/2023 – GdR MecaWave 2023

Commissariat à l'énergie atomique et aux énergies alternatives - www.cea.fr

Institut national de recherche en sciences et technologies du numérique - www.inria.fr

Institut Polytechnique de Paris - www.ip-paris.fr

Guided Waves for Structural Health Monitoring – gw4shm.eu



Context

- **Context:**
 - Modeling and Simulation for NDT, in particular SHM.
 - SHM: Environmental and Operational conditions (EOCs).
Mechanical loading conditions *in situ*. [Gorgin et al. 2020](#)
- **Colloque GdR MecaWave 2021 (direct model):**
Combining shell elements and transient spectral finite elements for guided wave propagation problems in prestressed thin structures.
- **Objective:**
Propose an inverse strategy to reconstruct loading conditions using ultrasonic guided waves measurements.
 - Direct model: Linearized elastodynamic model solved using 3D Spectral Finite Elements. [Dalmora et al. 2022](#)
 - Inversion: Iterated Unscented Kalman Filtering.

Slide 1

DA1 Notes:

- Pass sometime explaining (why, what, how) you are presenting.
- Always put references
- Do one repetition
- Be sure that the content will be explainable

DALMORA Andre; 05/07/2021



- The pipe is subjected to a force of 220kN which oscillates up to 2Hz.
- A weld with a defect is located between the transducer rings.
- The effect of prestresses significantly reduced the probability of detection of the defect.

Test stand of 4-point bending tests at IMA Dresden GmbH within the project QuantSHM (funding code 100207022) which was funded by the federal state of Saxony via the Sächsische Aufbaubank. (Image provided by Fraunhofer IKTS, a partner in the GW4SHM project.)

3

Input



Mechanical loading
causing deformation
+ Ultrasonic Source



Measurements by sparse
ultrasonic transducers

Direct Model

Inversion Algorithm

Output

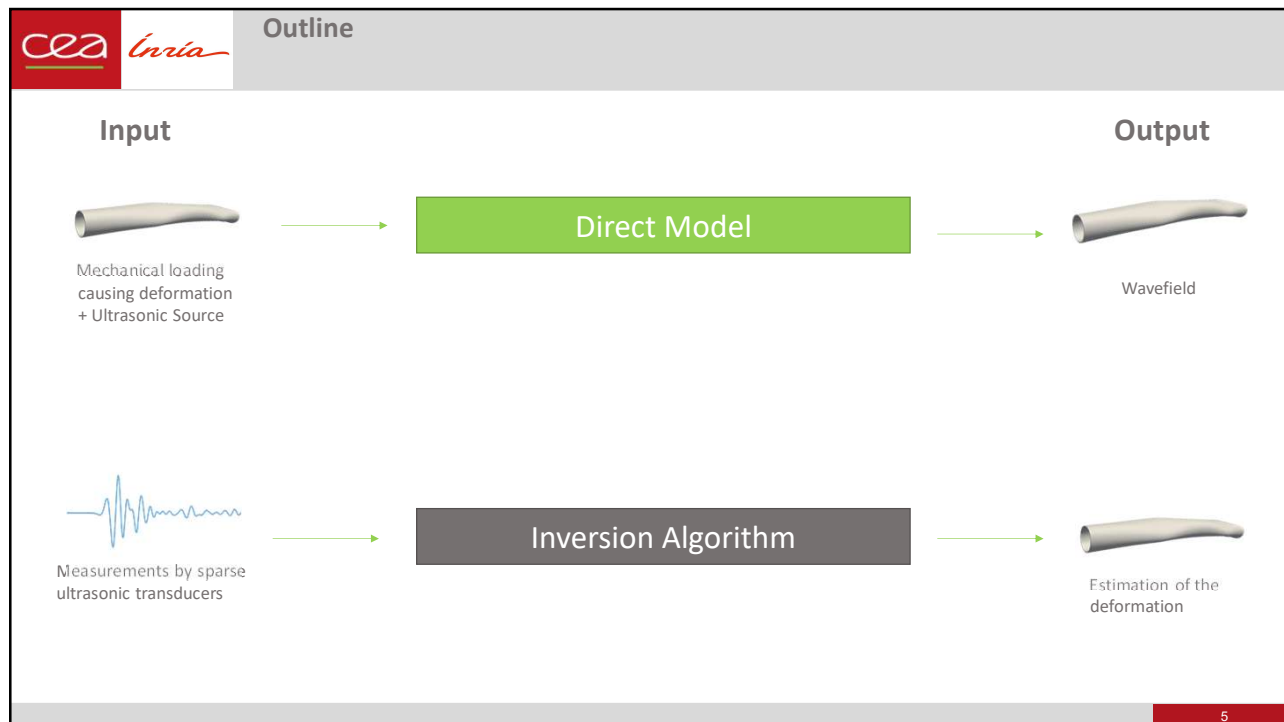


Wavefield



Estimation of the
deformation

4



cea Inria Direct model
Mechanical and Numerical modeling

Starting from the nonlinear elastodynamics in its strong formulation

$$\begin{cases} \rho \frac{\partial^2 \mathbf{u}}{\partial t^2} - \nabla_{\mathbf{x}} \cdot \boldsymbol{\sigma} = \rho \mathbf{f} & \text{on } \Omega(t), \\ \boldsymbol{\sigma} = \mathbf{G}(\mathbf{e}) & \text{(hyperelastic),} \\ \mathbf{u} = 0 & \text{on } \Gamma^D, \end{cases} \quad \text{with} \quad \mathbf{F} = \nabla_{\xi} \phi, \quad \mathbf{C} = \mathbf{F}^T \mathbf{F}, \quad \mathbf{e}(\mathbf{u}) = \frac{1}{2}(\mathbf{C} - \mathbf{1}).$$

6

Direct model

Method: Knowing that the associated forces differ in their natures, we decompose the problem in two sub-problems

$\hat{\Omega}$
 ξ

Ω_0
 X

$\Omega(t)$
 $x(t)$

scaled deformation (1e4)

u_0
 $f_0(\xi)$

\tilde{u}
 $\delta \tilde{f}(\xi, t)$

$f(\xi, t) = f_0(\xi) + \delta \tilde{f}(\xi, t)$
 $u(\xi, t)$

For $\delta \ll 1$, we look for
 $u(\xi, t) = u_0(\xi) + \delta \tilde{u}(\xi, t) + O(\delta^2)$,
 neglecting the terms of second order.

Modelling loaded wave propagation

Decomposition and numerical solving

Weak formulation $\forall w \in \mathcal{V}(\hat{\Omega})$

$$\frac{d^2}{dt^2} m[u, w] + a(u)[w] = l[w]$$

$$\begin{cases} m[u, w] = \int_{\hat{\Omega}} \hat{\rho} \mathbf{u} \cdot \mathbf{w} \, d\hat{\Omega}, \\ a(u)[w] = \int_{\hat{\Omega}} \boldsymbol{\Sigma}(\mathbf{e}) : \mathbf{D}_u \mathbf{e}(u)[w] \, d\hat{\Omega}, \\ l[w] = \int_{\hat{\Omega}} \hat{\rho} \mathbf{f} \cdot \mathbf{w} \, d\hat{\Omega}. \end{cases}$$

+

Linearization

$$f(\xi, t) = f_0(\xi) + \delta \tilde{f}(\xi, t)$$

$$u(\xi, t) = u_0(\xi) + \delta \tilde{u}(\xi, t) + O(\delta^2)$$

+ separating terms in δ

- **Structural deformation: Nonlinear and static.**

$a(u_0)[w] = l_0(w)$

- 3D Shell Finite Elements, avoiding numerical locking in thin structures. Chapelle and Bathe 2011
- MoReFEM code (MEDISIM - Inria team)

- **Wave propagation: Linearized and high frequency.**

$\frac{d^2}{dt^2} m[\tilde{u}, w] + D_u a(u_0)[\tilde{u}, w] = \tilde{l}[w]$

- Time domain (Explicit Leap Frog).
- SFEM kernel CIVA(CEA) Maday and Patera. 1989 ; Cohen 2002

Operators

$$m[u_0][w] = \int_{\hat{\Omega}} \boldsymbol{\Sigma}(\mathbf{e}_0) : \mathbf{D}_u \mathbf{e}(u_0)[w] \, d\hat{\Omega}$$

$$l_0[w] = \int_{\hat{\Omega}} \hat{\rho} \mathbf{f}_0 \cdot \mathbf{w} \, d\hat{\Omega}$$

$$m[\tilde{u}, w] = \int_{\hat{\Omega}} \hat{\rho} \tilde{\mathbf{u}} \cdot \mathbf{w} \, d\hat{\Omega},$$

$$D_u a(u_0)[\tilde{u}, w] = \int_{\hat{\Omega}} \mathbf{D}_u \mathbf{e}(u_0)[\tilde{u}] : \mathbf{D}_e \boldsymbol{\Sigma}(\mathbf{e}_0) : \mathbf{D}_u \mathbf{e}(u_0)[w] \, d\hat{\Omega} + \int_{\hat{\Omega}} \boldsymbol{\Sigma}(\mathbf{e}_0) : \mathbf{D}_e^2 \mathbf{e}[\tilde{u}, w] \, d\hat{\Omega},$$

$$\tilde{l}[w] = \int_{\hat{\Omega}} \hat{\rho} \tilde{\mathbf{f}} \cdot \mathbf{w} \, d\hat{\Omega}.$$

Remark on implementation $\forall w \in \mathcal{V}(\hat{\Omega}), \quad \frac{d^2}{dt^2} m[\tilde{u}, w] + D_u a(u_0)[\tilde{u}, w] = \tilde{l}[w]$

Discretizing by conform FE we have $\frac{d^2}{dt^2} M\vec{u} + K'(u_0)\vec{u} = \vec{f}$

Using a leapfrog time scheme $\vec{u}^{n+1} = -\Delta t^2 M^{-1} K'(u_0) \vec{u}^n + \Delta t^2 M^{-1} \vec{f} + 2\vec{u}^n - \vec{u}^{n-1},$

Lumped mass

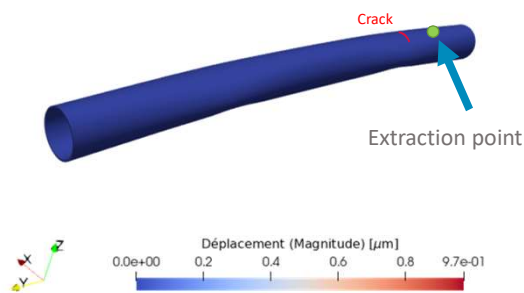
Parallelized non-assembled operation

Important aspects:

- Solving for **arbitrary hyperelastic constitutive law, geometry and mechanical loading.**
- High efficiency due to lumped-mass and parallelization.
- Non-assembled stiffness: low memory usage and inexpensive “parameter” update.
- Stability: operator non-negativeness must be assured.
- Strategy **validated** with experimental data.

9

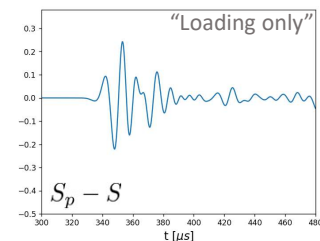
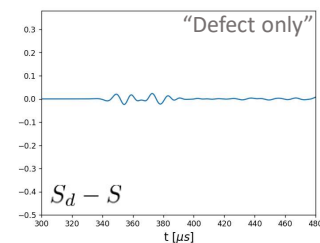
Wave propagation



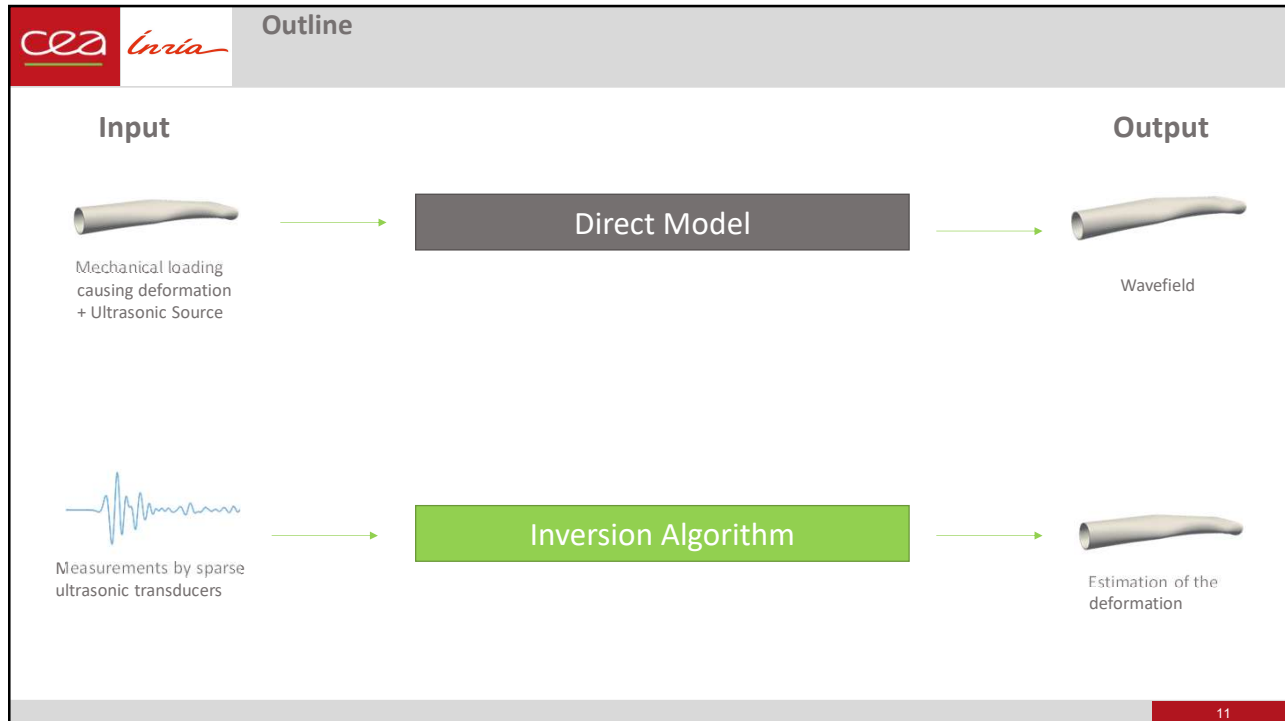
The effect of loading on wave propagation is evaluated numerically and compared with the effect of a defect. Considering the extracted simulated signals

- S : non deformed pipe (baseline; no defects).
- S_p : deformed pipe (without defect).
- S_d : pipe with defect (without deformation).

Effect of the defect vs prestresses



10



Loading condition reconstruction

Reconstructing loading deformation by means of limited ultrasonic measurements.

Direct model: $\frac{d^2}{dt^2}m[\tilde{u}, w] + D_u a(u_0)[\tilde{u}, w] = \tilde{l}(w)$

Objective: reconstruct u_0 using limited information over \tilde{u} .

We interpret the inverse problem as minimizing a least-squares misfit between measurements and data generated from the model.

Functional:

$$\mathcal{J}(u_0) = \min_{u_0} \frac{1}{2} \left\{ \|u_0\|_{\mathbb{P}_{p-1}}^2 + \frac{1}{N_s} \sum_i^{N_s} \int_0^T \|y_i(t) - C_i(\tilde{u}|_{u_0}(t))\|_{\mathbb{S}}^2 dt \right\}.$$

Annotations for the functional equation:

- number of measured signals (points to N_s)
- measurements (points to $y_i(t)$)
- Regularization norm (points to $\|u_0\|_{\mathbb{P}_{p-1}}^2$)
- observation operator (points to C_i)
- wavefield generated for the deformation u_0 (points to $\tilde{u}|_{u_0}(t)$)

It represents a nonlinear minimization problem.

3D model of a pipe showing: $\hat{\Omega}$, ξ , $\mathbf{u}_0 ?$, Ω_0 , X , $\tilde{\mathbf{u}}$, $\Omega(t)$, $x(t)$

12

Loading condition reconstruction

Remark on the dependency of direct problem

Direct model: $\frac{d^2}{dt^2} m[\tilde{u}, w] + D_u a(u_0)[\tilde{u}, w] = \tilde{l}[w]$

Dependency on u_0 (assuming know constitutive law and parameters):

$$D_u a(u_0)[\tilde{u}, w] = \int_{\hat{\Omega}} \underbrace{D_u e(u_0)[\tilde{u}] : D_e \Sigma(e_0) : D_u e(u_0)[w]}_{\text{"}\varepsilon(\tilde{u}) : C : \varepsilon(w)\text{"}} d\hat{\Omega} + \int_{\hat{\Omega}} \underbrace{\Sigma(e_0) : D_u^2 e[\tilde{u}, w]}_{\text{geometrical nonlinearity}} d\hat{\Omega}$$

Through the strain tensor and the stress tensor (for an arbitrary hyperelastic law):

$$D_e \Sigma = D_e^2 W = 4 \sum_{i=1}^n \frac{\partial W}{\partial I_i} \frac{\partial^2 I_i}{\partial C \partial C} + 4 \sum_{i,j=1}^n \frac{\partial^2 W}{\partial I_i \partial I_j} \frac{\partial I_i}{\partial C} \otimes \frac{\partial I_j}{\partial C}$$

Descent methods such as Full Waveform Inversion requires the tangent dynamics for computing an adjoint model. [Virieux et al. 2014](#)

Further differentiation of our direct model would require unwieldy operators as

$$D_e^3 W = 8 \sum_{i,j,k=1}^n \left[\frac{\partial^3 W}{\partial I_i \partial I_j \partial I_k} \frac{\partial I_i}{\partial C} \otimes \frac{\partial I_j}{\partial C} \otimes \frac{\partial I_k}{\partial C} \right] + 8 \sum_{i,j,k=1}^n \frac{\partial^2 W}{\partial I_i \partial I_j} \left[\frac{\partial^2 I_i}{\partial C \partial C} \otimes \frac{\partial I_j}{\partial C} + \dots \right].$$

Derivative-free methods are preferred.

13

Loading condition reconstruction

Remark on the parametric space to be reconstructed

Direct model: $\frac{d^2}{dt^2} m[\tilde{u}, w] + D_u a(u_0)[\tilde{u}, w] = \tilde{l}[w]$

The deformation sought u_0 is the result of a mechanical loading / solution of a quasi-static nonlinear problem

$$a(u_0)[w] = l_0(w).$$

Decomposing the deformation with the eigenmodes of $a(0)$

$$u_0(\xi) = \sum_{i=1}^{N_\theta} u_{i,0} \Psi_i(\xi)$$

we can significantly reduce the size of the parametric space to be reconstructed by reconstructing the coefficients $u_{i,0}^{(i)}$ with $N_\theta \ll$ Number of DoFs.

The parametric space is reduced and a selection of eigenmodes can be made from a first guess or sensitivity analysis.

14

Loading condition reconstruction

Variational Method

$$\begin{cases} \frac{d}{dt}p(t) + D_u A^* p(t) = -D_u C^*(y(t) - C(\tilde{u}(t))), \\ p(T) = 0, \end{cases}$$

$$D\mathcal{J}(u_0) = \mathbb{P}_{u_0}^{-1}u_0 - p(0).$$

Sequential Method

$$\begin{cases} \frac{d}{dt}\hat{z}(t) = A(\hat{z}(t)) + G(t)(y(t) - C(\tilde{u}(t))), \\ \hat{z}(0) = z_0, \end{cases}$$

$$z(T)$$

- With a reduced parametric space, the **Reduced Order Unscented Kalman Filter (ROUKF)** was chosen as the derivative-free method.
- Seem as a derivative-free version of the Extended Kalman Filter, where the propagation of the covariance is done empirically instead of applying the tangent dynamics.

15

Reduced-Order Unscented Kalman Filter

Sampling: $Z_n^{(i)+} = Z_n^+ + L_n \sqrt{U_n^{-1}} I^{(i)} \quad i \in [1, N_\theta + 1]$

Prediction:

$Z_n^{(1)+}$
 $\Psi_{n+1|n}(Z_n^{(1)+})$
 $Z_{n+1}^{(1)-}$

$Z_n^{(2)+}$
 $\Psi_{n+1|n}(Z_n^{(2)+})$
 $Z_{n+1}^{(2)-}$

\dots

$Z_n^{(N_\theta+1)+}$
 $\Psi_{n+1|n}(Z_n^{(N_\theta+1)+})$
 $Z_{n+1}^{(N_\theta+1)-}$

Correction:

$$\begin{aligned} Z_{n+1}^- &= E_\alpha(Z_{n+1}^{(i)-}) \\ L_{n+1} &= [Z_{n+1}^{*-}] D_\alpha [I^*]^\top \\ U_{n+1} &= \mathbb{1} + (CL)_{n+1}^* (CL)_{n+1} \\ Z_{n+1}^+ &= Z_{n+1}^- \\ &\quad + L_{n+1} U_{n+1}^{-1} (CL)_{n+1}^* (y_{n+1} - CE_\alpha(Z_{n+1}^{*+})) \end{aligned}$$

Extended state:

$$Z_n = \begin{pmatrix} \tilde{u}_n \\ \tilde{v}_n \\ \tilde{u}_{0,n} \end{pmatrix}$$

Forward operator:

$$\Psi_{n+1|n}(Z_n)$$

Covariance:

$$U^{-1}$$

Particles matrix:


$$[Z_n^*] = \begin{pmatrix} Z_n^{(1)} & Z_n^{(2)} & \dots & Z_n^{(N_\theta+1)} \end{pmatrix}$$

Sigma points and weights matrix:

$$[I^*] \quad D_\alpha = \begin{pmatrix} \alpha_1 & & & \\ & \ddots & & \\ & & \ddots & \\ & & & \alpha_{N_\theta+1} \end{pmatrix}$$

Moireau and Chapelle 2011

16



Reduced-Order Unscented Kalman Filter

Sampling: $Z_n^{(i)+} = Z_n^+ + L_n \sqrt{U_n^{-1}} I^{(i)}$ $i \in [1, N_\theta + 1]$

Prediction:

$Z_n^{(1)+}$
 $\Psi_{n+1|n}(Z_n^{(1)+})$
 $Z_{n+1}^{(1)-}$

$Z_n^{(2)+}$
 $\Psi_{n+1|n}(Z_n^{(2)+})$
 $Z_{n+1}^{(2)-}$

\dots

$Z_n^{(N_\theta+1)+}$
 $\Psi_{n+1|n}(Z_n^{(N_\theta+1)+})$
 $Z_{n+1}^{(N_\theta+1)-}$

Correction:

$$Z_{n+1}^- = E_\alpha(Z_{n+1}^{(i)-})$$

$$L_{n+1} = [Z_{n+1}^{*-}] D_\alpha [I^*]^\top$$


$$U_{n+1} = \mathbb{1} + (CL)_{n+1}^* (CL)_{n+1}$$

$$Z_{n+1}^+ = Z_{n+1}^- + L_{n+1} U_{n+1}^{-1} (CL)_{n+1}^* (y_{n+1} - CE_\alpha(Z_{n+1}^{*+}))$$

- Uncertainty only in u_0 .
- Iteration by time-step.
- Particles are evaluated in parallel.
- Propagates the covariance.

Moireau and Chapelle 2011

17



Reduced-Order Unscented Kalman Filter

Sampling: $Z_n^{(i)+} = Z_n^+ + L_n \sqrt{U_n^{-1}} I^{(i)}$ $i \in [1, N_\theta + 1]$

Prediction:

$Z_n^{(1)+}$
 $\Psi_{n+1|n}(Z_n^{(1)+})$
 $Z_{n+1}^{(1)-}$

$Z_n^{(2)+}$
 $\Psi_{n+1|n}(Z_n^{(2)+})$
 $Z_{n+1}^{(2)-}$

\dots

$Z_n^{(N_\theta+1)+}$
 $\Psi_{n+1|n}(Z_n^{(N_\theta+1)+})$
 $Z_{n+1}^{(N_\theta+1)-}$

Correction:

$$Z_{n+1}^- = E_\alpha(Z_{n+1}^{(i)-})$$

$$L_{n+1} = [Z_{n+1}^{*-}] D_\alpha [I^*]^\top$$

$$U_{n+1} = \mathbb{1} + (CL)_{n+1}^* (CL)_{n+1}$$

$$Z_{n+1}^+ = Z_{n+1}^- + L_{n+1} U_{n+1}^{-1} (CL)_{n+1}^* (y_{n+1} - CE_\alpha(Z_{n+1}^{*+}))$$



- Eigenmodes are stored and the non-assembled aspect allows inexpensive change of parameter.
- Attention must be given to the range explored by the particles to assure stability. This is done when choosing the initial covariance.

$$U_0 = \mathbb{P}_{u_0}$$

The initial components covariance of the set of eigenmodes are chosen from a u_0 a priori.


Moireau and Chapelle 2011

18

Loading condition reconstruction

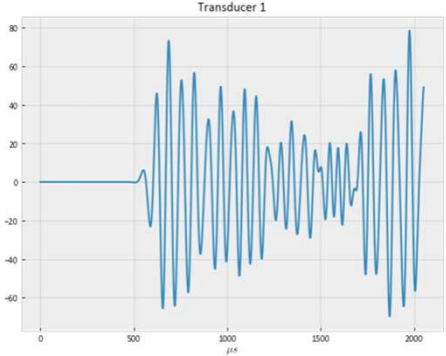
Study Cases



Transducers, natural state and target deformed state.
(300x deformation scale)



- Dimensions: 600 x 300 x 6.35 mm
- Measurements: 5 integration patches (radial).
- Excitation: 200kHz 5-cycles.
- Noise: 0.1%
- 180μs simulation time.
- 120 Smallest eigenvalues pairs computed.

Example of measured signal:




Obs. operator:
$$C_i(\tilde{\mathbf{u}}(t)) = \int_{\Gamma_i} \tilde{\mathbf{u}}(t) \cdot \mathbf{s}_i \, d\Gamma, \quad i \in [1, 5]$$

19

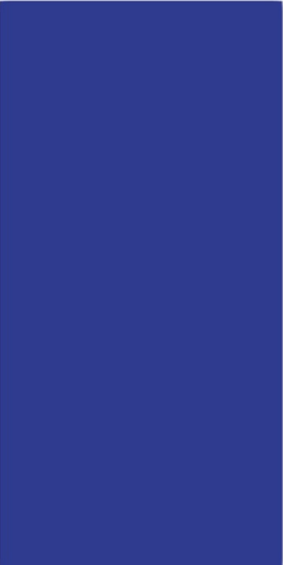



Loading condition reconstruction

Study Cases

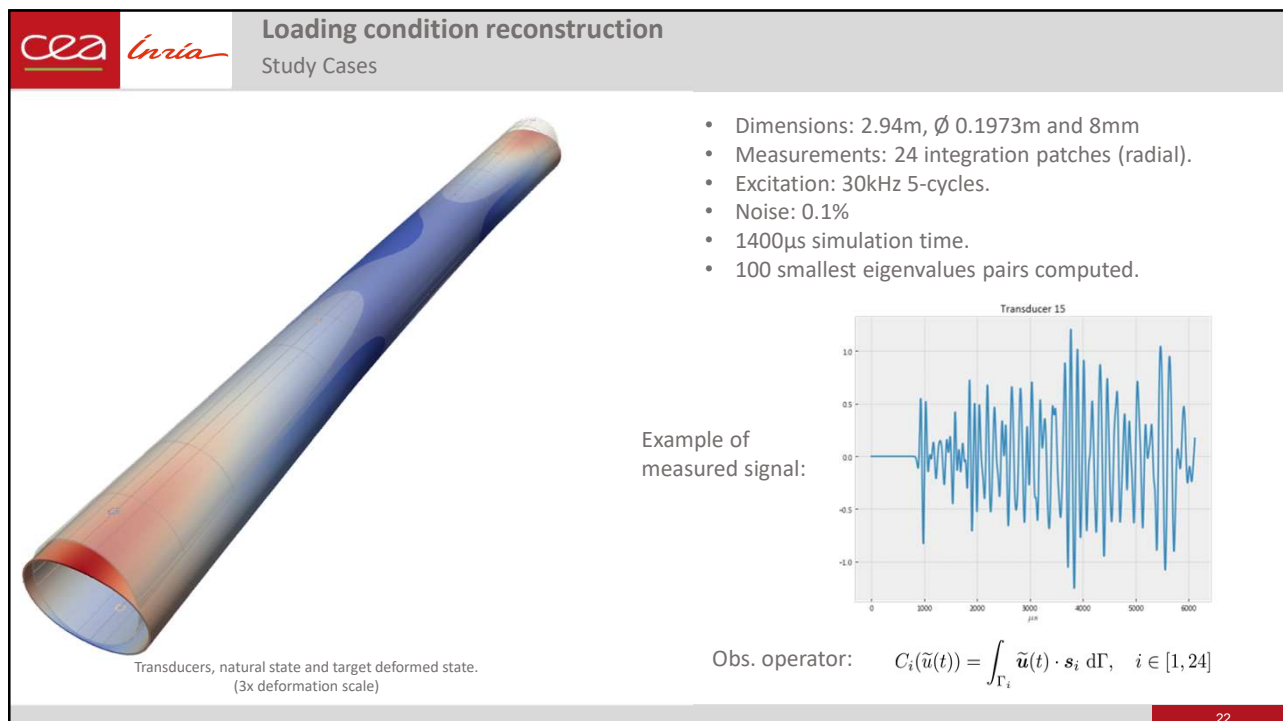
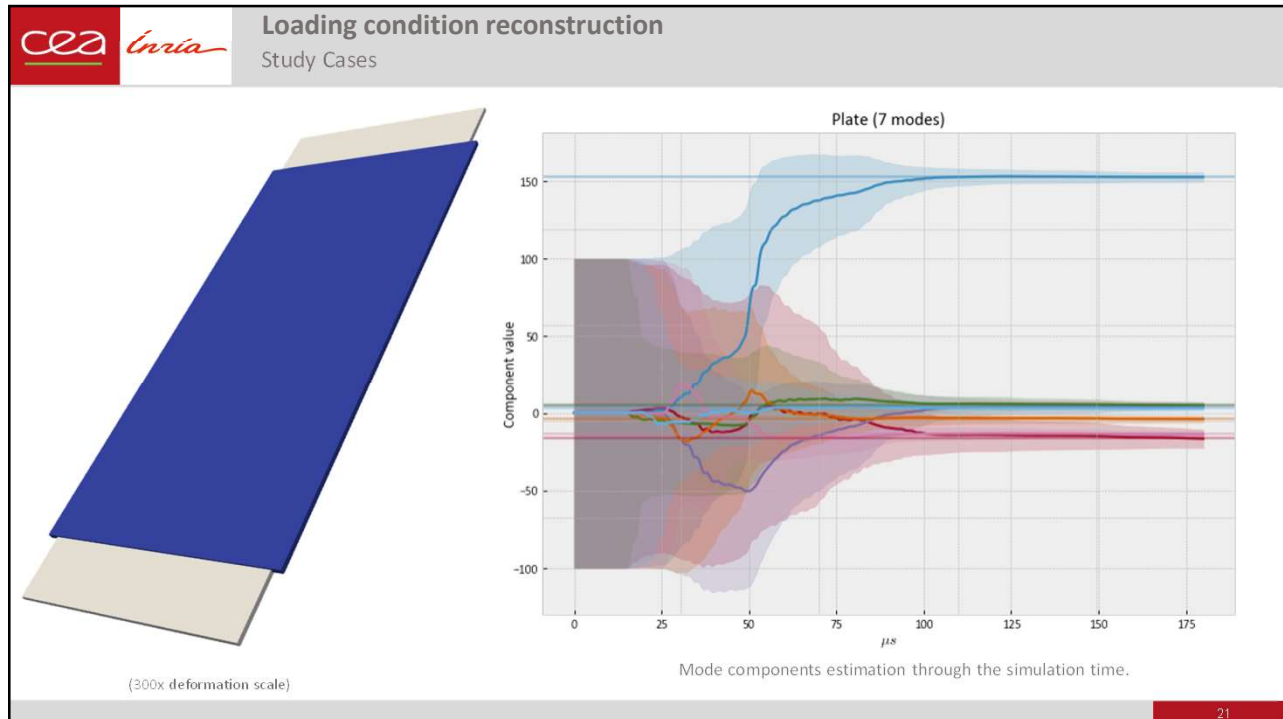


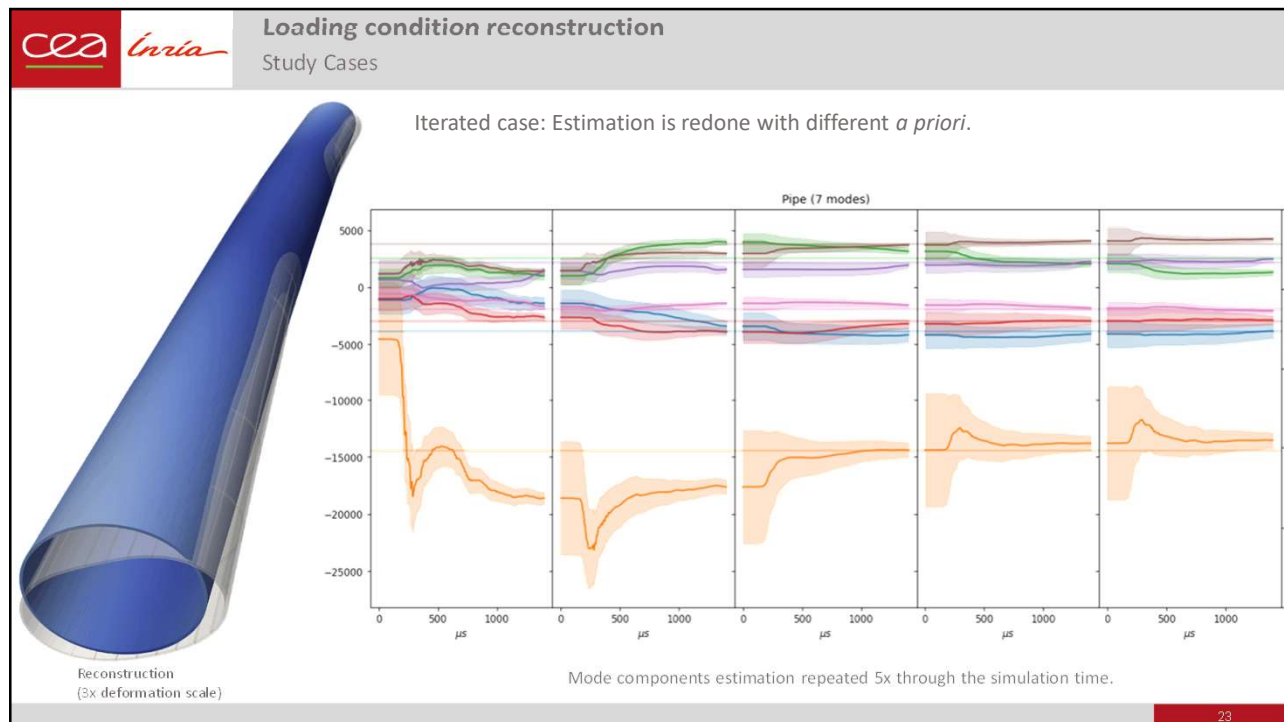
Transducers, natural state and target deformed state.
(300x deformation scale)



Target wavefield

20





cea Inria

Conclusions and Perspectives

Conclusions

- A **mechanical and numerical model** was presented for **wave propagation on loaded structures**. It comprises arbitrary hyperelastic law and non-buckling load.
- The simulation model was **validated using experimental data**.
- **Reconstruction of loading deformation** of the structure is done using the presented direct model and **Reduced order Kalman Filter (ROUKF)**.
- Reconstruction of loading deformation on realistic cases were presented.

Perspectives

- Further studies on the stability of the model and limitation of search range of estimator to **mitigate instability** during inversion.
- Mode selection: **sensitivity analysis** from estimation using observed data; different base with the *a priori*.

24

- Alexandre Imperiale, and Edouard Demaldent. 2019. "A Macro-Element Strategy Based upon Spectral Finite Elements and Mortar Elements for Transient Wave Propagation Modeling. Application to Ultrasonic Testing of Laminate Composite Materials." *International Journal for Numerical Methods in Engineering* 119 (10): 964–90.
- Chapelle, Dominique, Anca Ferent, and K. Bathe. 2004. "3D-Shell Elements and Their Underlying Mathematical Model." *Mathematical Models and Methods in Applied Sciences* 14.
- Cohen, Gary C. 2002. *Higher-Order Numerical Methods for Transient Wave Equations*. 1st edition. Scientific Computation. Berlin Heidelberg: Springer-Verlag.
- Dalmora, André, Alexandre Imperiale, Sébastien Imperiale, and Philippe Moireau. 2022. "A Generic Numerical Solver for Modeling the Influence of Stress Conditions on Guided Wave Propagation for SHM Applications." In . American Society of Mechanical Engineers Digital Collection.
- Gandhi, Navneet, Jennifer E Michaels, and Sang Jun Lee. 2012. "Acoustoelastic Lamb Wave Propagation in Biaxially Stressed Plates." *The Journal of the Acoustical Society of America* 132 (3): 1284–93.
- Joly, Patrick. 2007. "Numerical Methods for Elastic Wave Propagation." In *Waves in Nonlinear Pre-Stressed Materials*, edited by Michel Destrade and Giuseppe Saccomandi, 181–281. CISM Courses and Lectures. Vienna: Springer.
- Maday, Yvon, and Anthony T. Patera. 1989. *Spectral Element Methods for the Incompressible Navier-Stokes Equations*.
- Moireau, Philippe, and Dominique Chapelle. 2011. "Reduced-Order Unscented Kalman Filtering with Application to Parameter Identification in Large-Dimensional Systems." *ESAIM: Control, Optimisation and Calculus of Variations* 17 (2): 380–405.
- Virieux, J., A. Asnaashari, R. Brossier, L. Métivier, A. Ribodetti, and W. Zhou. 2014. "6. An Introduction to Full Waveform Inversion." In *Encyclopedia of Exploration Geophysics*, R1-1-R1-40. Geophysical References Series. Society of Exploration Geophysicists.

This research was funded by the following project: "GW4SHM" (gw4shm.eu) project from the European Union's Horizon 2020 Research and Innovation program under the Marie Skłodowska-Curie, grant number 860104.